Mechanism of Presynaptic Filament Stabilization by the Bacteriophage T4 UvsY Recombination Mediator Protein†

Jie Liu,‡ Jeffrey P. Bond,§,|| and Scott W. Morrical*,‡,§,||

Department of Biochemistry, Department of Microbiology and Molecular Genetics, and Vermont Cancer Center, University of Vermont College of Medicine, Burlington, Vermont 05405

Received December 9, 2005; Revised Manuscript Received February 14, 2006

ABSTRACT: UvsY is the recombination mediator protein (RMP) of bacteriophage T4, which promotes homologous recombination by facilitating presynaptic filament assembly. The results of previous studies suggest that UvsY promotes the assembly of presynaptic filaments in part by stabilizing interactions between T4 UvsX recombinase and single-stranded DNA (ssDNA). To test this hypothesis, we studied the interactions of UvsX and UvsY with a fluorescein-derivatized oligonucleotide. This assay distinguishes between bipartite UvsX− or UvsY−ssDNA and tripartite UvsX−UvsY−ssDNA complex formation via differential fluorescence quenching effects. Salt stabilities of the three complexes were measured at equilibrium in the presence and absence of various nucleotide ligands of the UvsX protein and also under steady-state conditions for UvsX-catalyzed ssDNA-dependent ATP hydrolysis. The results demonstrate that UvsY globally stabilizes UvsX−ssDNA complexes, consistent with an increase in the apparent equilibrium binding affinity, $K_{ss}\omega$, of the UvsX−ssDNA interactions. The UvsY-mediated affinity increase is observed at equilibrium in the presence of ADP, ATPγS, or in the absence of the nucleotide and also at steady-state in the presence of ATP. Intriguingly, the stabilizing effects of UvsY and ATPγS on UvsX−ssDNA interactions are synergistic, indicating nonredundant mechanisms for UvsX−ssDNA complex stabilization by RMP versus nucleoside triphosphate effectors. Experiments with UvsY missense mutants defective in ssDNA binding demonstrate that UvsY−ssDNA interactions are of major importance in stabilizing UvsX−ssDNA complexes, whereas UvsY−UvsX protein−protein interactions provide residual stabilization energy. Together, the data is consistent with a mechanism in which UvsY stabilizes presynaptic filaments by organizing the ssDNA lattice into a structure that is favorable for UvsX−ssDNA interactions.

Homologous recombination events are catalyzed by nucleoprotein structures called presynaptic filaments that contain recombination proteins bound to single-stranded DNA (ssDNA[1]). Presynaptic filaments catalyze DNA strand exchange reactions that initiate recombination-dependent DNA replication (RDR) and recombinational DNA repair pathways, that is, double-strand break repair or DSBR (*1*−*6*). The proper assembly of presynaptic filaments is critical for productive recombination/repair, and the disruption of filament assembly pathways are associated with human disease states (*7*−*11*). Core functionalities in the assembly and activity of presynaptic filaments are conserved in all kingdoms of life and include general recombinases of the RecA family, recombination mediator proteins (RMPs), and ssDNA-binding proteins (SSBs) (*12*), among others. In each organism, these proteins together with their functional partners must bring about the targeted assembly of recombinase filaments onto ssDNA while mitigating the competition for recombinase−ssDNA interactions by other factors.

Recombination systems face two major challenges during presynaptic filament assembly: First is the competition between the SSB and the recombinase components for binding sites on ssDNA, which is responsible for the profound protein order of addition effects observed in the in vitro DNA strand exchange reactions of many systems (*13*−*19*). Second is the inability of many recombinases to effectively discriminate between ssDNA and dsDNA lattices, resulting in the inhibition of recombinase functions under conditions of excess dsDNA, as occurs in the cell (*20*−*22*). Recombination mediator proteins are important for overcoming the competitive effects of SSBs (*12*) and may also be important for targeting recombinase assembly onto ssDNA as opposed to dsDNA lattices (*23*).

Studies of the bacteriophage T4 homologous recombination system have yielded important insights on the biochemistry of presynaptic filament assembly, and indicate some of the mechanisms used to overcome competitive challenges to filament assembly posed by SSBs and dsDNA (*17*, *24*−

† This work was supported by NIH Grant no. GM48847 to S.W.M., by NCI grant no. CA022935 to the Vermont Cancer Center, and by an NIH NCRR grant to the Vermont Genetics Network. J.L. was supported by a DOE-EPSCoR predoctoral fellowship in structural biology.

* To whom correspondence should be addressed. Tel: 802-656-8260. Fax: 802-656-8220. E-mail: smorrica@uvm.edu.

‡ Department of Biochemistry.

§ Department of Microbiology and Molecular Genetics.

|| Vermont Cancer Center.

[1] Abbreviations: ssDNA, single-stranded DNA; dsDNA, double-stranded DNA; RDR, recombination-dependent replication; RMP, recombination mediator protein; SSB, single-stranded DNA binding protein; HPSF, high purity salt free; ATPγS, adenosine-5′-(γ-thio)-triphosphate; ϵDNA, etheno-modified random sequence ssDNA; $12FdT_{24}$, oligonucleotide dT_{24}-containing fluorescein moiety attached to the 12th nucleotide residue from the 5′ end.

10.1021/bi0525167 CCC: $33.50
Published on Web 04/07/2006

27). The three major proteins involved in the T4 presynapsis are the UvsX recombinase, UvsY recombination mediator protein, and Gp32 ssDNA-binding protein. A biochemical model has emerged (*3*, *12*) in which Gp32 prepares the ssDNA for filament assembly through cooperative, high-affinity binding. This binding not only eliminates inhibitory secondary structures in the lattice but also interferes with UvsX loading through competitive effects (*26*). UvsY protein eliminates this competition by binding to the Gp32−ssDNA complex and weakening it, preparing the Gp32 for displacement by UvsX. UvsX filament assembly then nucleates and propagates on the UvsY−Gp32−ssDNA intermediate in the presence of ATP, displacing Gp32 in the process. This model accounts for two of the major properties of UvsY protein inferred from biochemical studies: the ability to destabilize Gp32−ssDNA interactions (*27*) and the ability to stabilize UvsX−ssDNA interactions (*25*).

Indirect evidence for the stabilization of UvsX−ssDNA filaments by UvsY comes from observations that UvsY decreases the salt-inhibition of UvsX-catalyzed, ssDNA-dependent ATPase and DNA strand exchange reactions (*25*, *29*, *30*). The mechanism of this stabilization is unknown; UvsY could induce an increase in the affinity ($K_{ss}\omega$) of UvsX for ssDNA, or it could merely act as a glue to hold the filament together by means of its own strong interactions with UvsX and ssDNA (*28*, *29*). Direct evidence exists for the destabilization of Gp32−ssDNA complexes by UvsY, and this destabilization was shown to be independent of UvsY−Gp32 protein−protein interactions (*27*). A structural change in ssDNA induced by UvsY, possibly related to the wrapping of the polynucleotide around the UvsY hexamers, is proposed to be responsible for the destabilization of Gp32−ssDNA interactions (*27*, *31*). Conceivably, the stabilization of UvsX−ssDNA interactions by UvsY could be mediated by similar structural changes in ssDNA, by UvsX−UvsY protein−protein interactions, or both. At the same time, the poorly hydrolyzed ATP analogue, ATPγS, stabilizes UvsX−ssDNA complexes, at least, in part by increasing the intrinsic affinity (K_{ss}) of the interaction (*23*, *32*). UvsY could mimic the effects of ATPγS, or it could work by an independent mechanism.

To address the mechanism of presynaptic filament stabilization by the UvsY protein, we performed fluorescence studies of UvsX and UvsY interactions with a fluorescein-labeled oligonucleotide, $12FdT_{24}$. The results showed that UvsX, UvsY, and UvsX−UvsY complexes with $12FdT_{24}$ could be resolved by differential fluorescence-quenching effects, allowing us to study the salt-stabilities of the three complexes in the presence and absence of various nucleotide ligands of UvsX. Using this method, we determined that UvsY has a global stabilizing effect on UvsX−ssDNA interactions, consistent with an increase in the apparent equilibrium binding affinity of UvsX for ssDNA under all conditions. Stabilizing effects of UvsY and ATPγS on UvsX−ssDNA interactions are synergistic, indicating non-redundant mechanisms for stabilization by mediator and nucleoside triphosphate effectors. The stabilizing effect of UvsY depends strongly on UvsY−ssDNA interactions, consistent with a model in which ssDNA structural changes induced by UvsY create an optimal lattice for the UvsX−ssDNA filament assembly. The thermodynamic stabilization of UvsX−ssDNA interactions by UvsY and nucleoside triphosphate likely plays a major role in overcoming SSB and dsDNA inhibition effects during homologous recombination and RDR transactions.

MATERIALS AND METHODS

Reagents and Buffers. All chemicals used were reagent grade, and the aqueous solutions were made with water purified through a Barnstead system. ADP, AMP, ATPγS, and ATP were purchased from Sigma. Buffer A, used in the fluorescence studies, contained 20 mM Tris-HCl at pH 7.4, 2 mM $MgCl_2$, and variable concentrations of NaCl. Buffer B, used in ATPase studies, contained 20 mM Tris-HCl at pH 7.4, 90 mM KCl, and 10 mM $MgCl_2$. All protein storage buffers were as described (*28*, *32*).

Proteins and Nucleic Acids. Recombinant T4 UvsX (44 kDa), wild-type UvsY (15.8 kDa), and two UvsY mutant proteins ($UvsY_{K58A}$ and $UvsY_{K58A,R60A}$) were purified, stored, and shown to be nuclease-free, according to published procedures (*28*, *30*, *33*, *34*). Extinction coefficients for UvsX and UvsY sp. at 280 nm were 69 760 $M^{-1}cm^{-1}$ and 19 180 $M^{-1}cm^{-1}$, respectively (*28*, *30*, *32*).

The HPSF-purified ssDNA oligonucleotide $12FdT_{24}$, containing a fluorescein moiety conjugated to the 12th dT residue from the 5′-end, was purchased from MWG-Biotech (High Point, NC). Its concentration was determined by the absorbance at 260 nm using a molar extinction coefficient of 211 499 $M^{-1}cm^{-1}$ as provided by the manufacturer. All DNA concentrations are given in nucleotide residues.

Fluorescence Assays. All fluorescence data were collected on a Quantamaster QM-4 fluorometer (Photon Technology International, South Brunswick, NJ). This fluorometer was equipped with a 75-W Xenon arc lamp as an excitation source and excitation/emission monochromators to measure steady-state fluorescence. All of the data was collected in the steady-state mode and corrected for effects of dilution, solution change, photobleaching, inner filter effects, and intrinsic protein fluorescence as described (*32*, *35*, *36*). For salt-back-titrations, mock experiments were carried out using the same components without the proteins to correct for photobleaching, dilution, and solution change. The samples were only exposed to the beam during data acquisition mode to minimize photobleaching. All of the experiments were performed at room temperature with a starting volume of 700 μL. The emission spectra, collected from 500 to 540 nm, were the averages of three independent scans at an excitation wavelength of 465 nm. In titration experiments, each data point equals the average of 30 readings at an emission wavelength of 519 nm with an excitation wavelength of 465 nm. The slit widths for excitation and emission were 1 and 5 nm, respectively. A long pass-cutoff glass filter at 495 nm was used for all of the emission data collection.

Forward stoichiometric titrations were used to determine the binding-site size (n) for UvsX on $12FdT_{24}$, with or without UvsY. To obtain the n value without UvsY, the reactions were carried out in buffer A plus 10 mM NaCl. $12FdT_{24}$ (0.8 μM) was preincubated in the buffer, and then aliquots of concentrated UvsX stock solution were sequentially added to the solution. To obtain the n value for UvsX in the presence of UvsY, the reactions were carried out in buffer A plus 100 mM NaCl (to prevent protein precipitation). $12FdT_{24}$ (1.0 μM) and UvsY (0.25 μM) were prein-

cubated in the buffer, and then aliquots of concentrated UvsX stock solution were sequentially added to the solution. The ionic strength of the UvsX stock solution was adjusted to match the ionic strength of the starting reaction buffer by dilution. Control experiments included mock titrations without $12FdT_{24}$ or UvsX (replaced with UvsX storage buffer) to correct for dilution effects, photobleaching, solution change, inner filter effects, and protein fluorescence contributions.

Salt-back-titrations were used to determine the relative stabilities of protein−DNA complexes. In all of the reactions, a 1:1 (protein monomers/ssDNA binding sites, assuming a binding-site size of $n = 4$ nucleotide residues per UvsY monomer or per UvsX monomer (*28*, *32*)) protein−DNA complex was allowed to pre-equilibrate in buffer A plus 100 mM NaCl. All reactions contained 2 μM $12FdT_{24}$ with 0.5 μM UvsX, 0.5 μM UvsY, or 0.5 μM UvsX plus 0.5 μM UvsY. The reactions involving UvsY mutants ($UvsY_{K58A}$ or $UvsY_{K58A,R60A}$) contained 0.5 μM of the mutant protein alone or in combination with 0.5 μM UvsX. To compare the effects of different nucleotides on the formation and stability of protein−DNA complexes, some reaction systems contained 1 mM ADP, 1 mM ATPγS, or an ATP-regenerating system consisting of 1 mM ATP, 5 mM phosphoenolpyruvate, and 2.6 units/mL pyruvate kinase. On the basis of previous studies, buffer A plus 100 mM NaCl was chosen as the starting buffer to enhance complex solubility; UvsX and UvsY both form stoichiometric complexes with ssDNA at this salt concentration (*28*, *32*), although both UvsY mutants essentially lack ssDNA binding activity under the experimental conditions used (*30*). A 5 M stock solution of NaCl was used as the titrant to achieve different salt concentrations. Every salt-back-titration experiment had a corresponding mock experiment containing the same components without the protein to correct for photobleaching, dilution effects, and solution change. Independent experiments containing identical starting materials without $12FdT_{24}$ showed that protein fluorescence contributions were negligible.

Statistical Treatment of Salt-back Titration Data. Fluorescence measurements were analyzed using the R language and environment for statistical computing (*37*). Fluorescence data were fit using

$$\frac{F}{F_0} = L + R(1 - \theta) \quad (1)$$

where L and R are the low salt limit and response parameters, respectively, and θ is the fractional saturation of the lattice, which is given implicitly by

$$\log \frac{\theta}{(1-\theta)(P_T - \theta D_T)} = -\log (P_T - D_T/2) + \beta(\log[\mathrm{NaCl}] - x_{1/2}) \quad (2)$$

where P_T and D_T are the total protein and DNA concentrations, respectively, in the titration. Although the precise thermodynamic model for protein−DNA−salt interactions is not known, $x_{1/2}$ satisfactorily captures the mid-dissociation point and provides a statistic that allowed us to infer differences in the DNA-binding behavior of the proteins. Inference was based on the Wilcoxon rank sum test and Student's t-test.

ATPase Assays. A coupled spectrophotometric ATPase assay with a slight modification (*34*) was used to determine the ssDNA-dependent ATP hydrolysis rates of UvsX. Timecourses for all reactions were recorded on a Hitachi U-2000 spectrophotometer. A water-jacketed cuvette holder was used to maintain a constant temperature of 37 °C. All reactions were carried out in 1 mL quartz cuvettes of 1 cm path length with final reaction volumes of 700 μL. The reactions contained 0 or 2 μM $12FdT_{24}$, 0 or 0.5 μM UvsX, and 0 or 0.5 μM UvsY as indicated. The buffer for low salt reactions consisted of buffer B plus 2 mM ATP, 6 units/mL of pyruvate kinase, 6 units/mL of lactate dehydrogenase, 2.3 mM phosphoenolpyruvate, and 0.23 mM NADH. The buffers for the dissociation midpoint and high salt reactions were identical to that for the low salt reactions, except for the addition of 20−500 mM NaCl as indicated. All reaction components except UvsX protein were preincubated in the cuvette for 5 min at 37 °C, and then the reactions were initiated by adding UvsX. The linear portions of timecourses from the absorbance change at 380 nm were used to calculate ATP hydrolysis velocities as described (*34*).

RESULTS

Quenching of $12FdT_{24}$ Fluorescence by UvsX and UvsY Proteins. Fluorescent derivatives of the oligonucleotide dT_{24} were chosen to study the effects of UvsY on UvsX−ssDNA interactions. The 24-mer was chosen because it contains binding sites for six UvsX protomers and ±6 UvsY protomers, on basis of the binding site sizes of $n = 4$ nucleotide residues for each (*28*, *32*). The UvsX-saturated 24-mer represents at least one helical turn of the presynaptic filament (Discussion). In addition, dT_{24} forms a discrete 1:1 complex with hexameric UvsY protein (*31*), and therefore, the length of this lattice is ideal for measuring the interactions of UvsX with a minimal UvsY−ssDNA complex, such as may be encountered during nucleation and/or early propagation stages of presynaptic filament assembly.

Single fluorescein conjugates of oligonucleotide dT_{24} undergo fluorescence quenching upon binding by UvsX and/or UvsY proteins (Figure 1). The degree of quenching varies with the position of the fluorophore (data not shown); we observed maximum quenching when fluorescein was attached to the 12th dT residue from the 5′ end. Therefore, this conjugate, $12FdT_{24}$, was used for all subsequent experiments. Figure 1 shows the fluorescence spectra of $12FdT_{24}$ in the presence/absence of saturating concentrations of UvsX, UvsY, or both. UvsX alone quenches $12FdT_{24}$ fluorescence by approximately 15% measured at 519 nm, whereas UvsY alone causes 12% quenching. Interestingly, adding an equimolar amount of UvsX to the UvsY−$12FdT_{24}$ complex causes an additional 8% quench of the fluorescein signal measured at the same emission wavelength (Figure 1). Note that the spectra of both UvsY-containing mixtures are red-shifted by 1−2 nm. The different quenching effects caused by UvsX in the presence vs absence of UvsY indicates that the formation of a maximally quenched, tripartite UvsX−UvsY−$12FdT_{24}$ complex can be differentiated from the formation of bipartite UvsX−$12FdT_{24}$ and UvsY−$12FdT_{24}$ complexes via fluorescence changes.

Maximally Quenched Complex Contains Enzymatically Active UvsX Protein. To verify that the maximally quenched

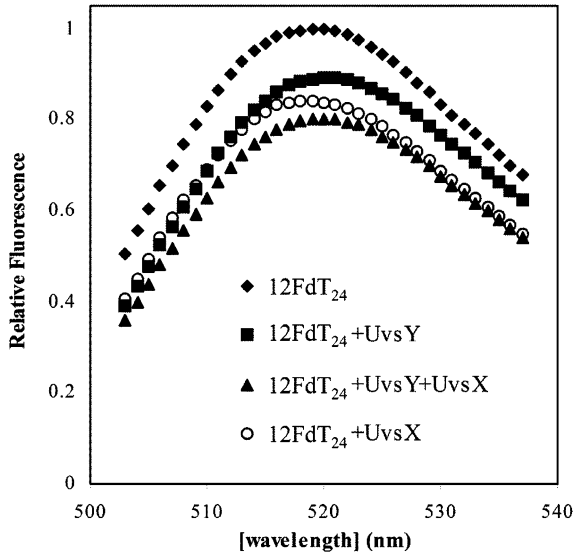

FIGURE 1: Fluorescence spectra of single-stranded oligonucleotide $12FdT_{24}$ in the presence and absence of UvsX, UvsY, or both proteins. All solutions contained 2 μM $12FdT_{24}$ in buffer A plus 100 mM NaCl. (♦) $12FdT_{24}$ alone; (○) $12FdT_{24}$ + 0.5 μM UvsX; (■) $12FdT_{24}$ + 0.5 μM UvsY; (▲) $12FdT_{24}$ + 0.5 μM UvsX + 0.5 μM UvsY. Fluorescence emission scans were collected as described in Materials and Methods, and each one represents the average of three independent scans. All data were normalized against the fluorescence emission signal for $12FdT_{24}$ alone at 519 nm. Protein amounts are at 1:1 stoichiometry with respect to ssDNA binding sites assuming a binding site size of $n = 4$ nucleotide residues per monomer of UvsX or UvsY.

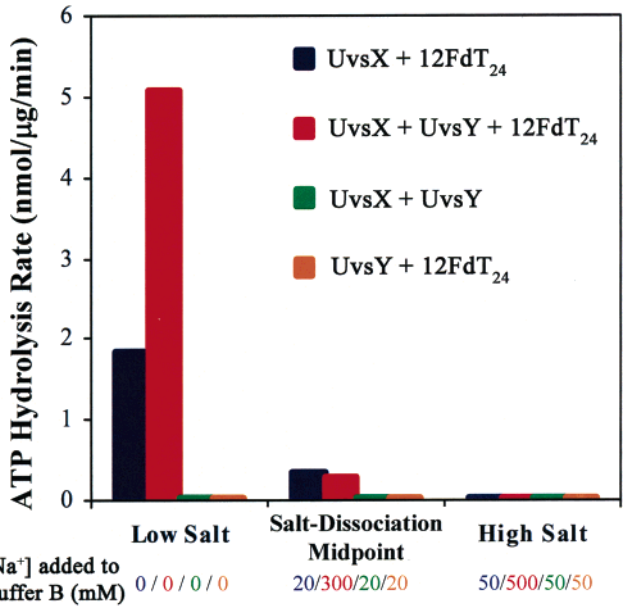

FIGURE 2: $12FdT_{24}$-stimulated ATPase activity of UvsX recombinase as functions of UvsY protein and salt. ATPase assays were performed as described in Materials and Methods. The reactions contained either 0.5 μM UvsX + 2 μM $12FdT_{24}$ (blue columns), 0.5 μM UvsX + 0.5 μM UvsY + 2 μM $12FdT_{24}$ (red columns), 0.5 μM UvsX + 0.5 μM UvsY (green columns), or 0.5 μM UvsY + 2 μM $12FdT_{24}$ (yellow columns). All reactions contained buffer B (20 mM Tris-HCl at pH 7.4, 90 mM KCl, and 10 mM $MgCl_2$) plus 2 mM ATP, 6 units/mL of pyruvate kinase, 6 units/mL of lactate dehydrogenase, 2.3 mM phosphoenolpyruvate, and 0.23 mM NADH. The reactions were supplemented with NaCl concentrations as indicated in the Figure.

complex contains UvsX, we measured UvsX-catalyzed, ssDNA-dependent ATPase rates in the presence of the $12FdT_{24}$ oligonucleotide and in the presence/absence of UvsY. The results are shown in Figure 2. Under low-salt conditions, $12FdT_{24}$ stimulates ATPase activity, demonstrating that this oligonucleotide is a sufficient lattice to support the UvsX enzymatic activity. The presence of UvsY increases the rate of UvsX ATPase activity by 2.5-fold under low-salt conditions, demonstrating that UvsX continues to bind to the oligo in the presence of UvsY and that UvsY provides its characteristic stimulation of UvsX enzymatic activities even on this restricted lattice (*17*, *25*, *38*). Increasing the salt concentration inhibits ATPase activity in a manner consistent with the disruption of UvsX−ssDNA interactions (Figure 2). We empirically determined the amounts of NaCl that when added to buffer B cause 50 or 100% loss of fluorescence quenching, indicative of protein−$12FdT_{24}$ complex dissociation (data not shown). For UvsX−$12FdT_{24}$ complexes, these amounts were 20 and 50 mM NaCl, respectively. For the maximally quenched complex, these amounts were 300 and 500 mM NaCl, respectively. At the 50% dissociation point for UvsX−$12FdT_{24}$, the ATPase velocity is decreased by 80% compared to that in low-salt conditions (Figure 2). A nearly identical ATPase velocity is obtained at the 50% dissociation point of the maximally quenched complex (Figure 2). Identical assays performed under high-salt conditions gave ATPase rates that were indistinguishable from the background (Figure 2). Therefore, the enzymatic activity of UvsX correlates with its association and dissociation from $12FdT_{24}$ both in the absence and presence of UvsY. Note that much higher salt concentrations are required to disrupt UvsX ATPase activity in the presence of UvsY than that required in its absence.

Binding Site Size of UvsX on 12FdT$_{24}$ in the Presence/Absence of UvsY. To determine the binding site size (n) value of UvsX on $12FdT_{24}$, forward titrations of the oligo with UvsX were carried out under low-salt, tight binding conditions. Plateau fluorescence quenching was achieved when all of the binding sites in the oligo had been saturated with protein. As shown in Figure 3A, at an oligo concentration of 0.8 μM (nucleotide residues), the plateau is attained at a UvsX concentration between 0.15 and 0.20 μM, indicating an apparent binding site size of $n = 4-5$ nucleotide residues, consistent with previous determination of $n = 4$ for UvsX binding to long etheno-modified ssDNA lattices (*32*). A similar experiment was performed to determine the binding site size of UvsX on a preformed UvsY−$12FdT_{24}$ complex (Figure 3B). Here, 1.0 μM $12FdT_{24}$ was preincubated with 0.25 μM UvsY, a stoichiometric amount assuming a binding site size of 4 nucleotide residues per UvsY monomer (*28*), resulting in an initial degree of fluorescence quenching (data not shown). The titration of this mixture with UvsX resulted in additional fluorescence quenching, representing the formation of the maximally quenched UvsX−UvsY−$12FdT_{24}$ complex. The plateau was attained at approximately 0.2 μM UvsX (Figure 3B), corresponding to a binding site size of $n = 5$ for UvsX. Thus, UvsX binds to the oligonucleotide $12FdT_{24}$ with a binding site size similar to that measured on long ssDNA lattices. The binding site size is similar in the presence or absence of UvsY, consistent with previous reports that UvsX and UvsY can co-occupy ssDNA (*25*, *38*, *39*).

Effects of Salt and Nucleotides on UvsX−UvsY−12FdT$_{24}$ Interactions. UvsX− and UvsY−ssDNA interactions are

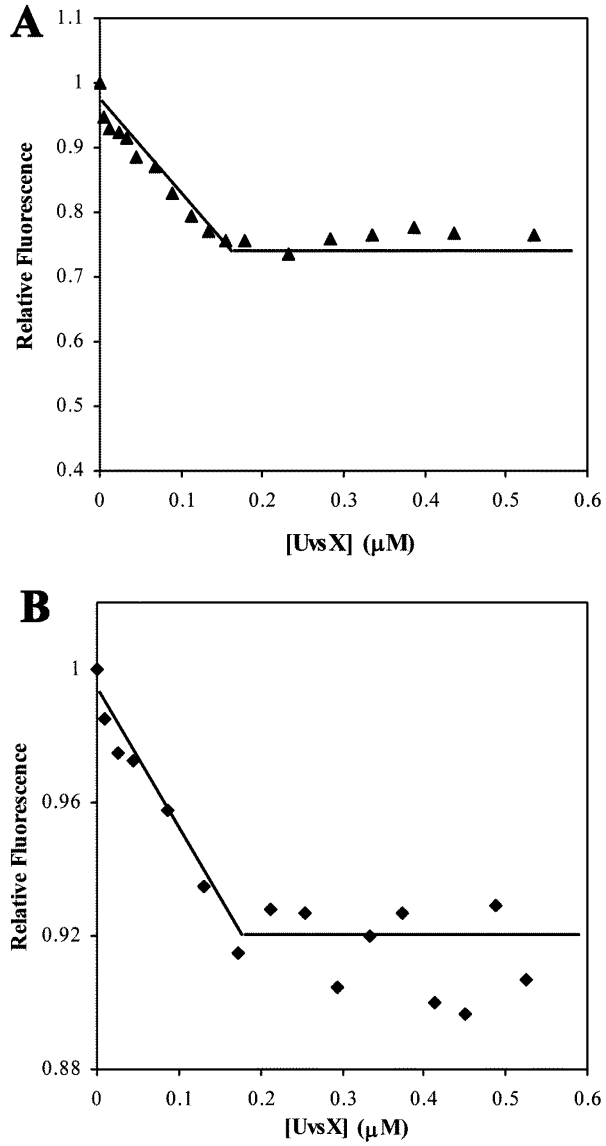

FIGURE 3: Titrations of $12FdT_{24} \pm$ UvsY protein with UvsX under tight binding conditions. Fluorescence titrations were performed as described in Materials and Methods. (A) Titration of 0.8 μM $12FdT_{24}$ with UvsX protein in buffer A + 10 mM NaCl. (B) Titration of a preincubated mixture containing 1.0 μM $12FdT_{24}$ + 0.25 μM UvsY with UvsX protein in buffer A + 100 mM NaCl.

highly electrostatic in nature and, therefore, salt-sensitive (*28*, *32*). Thus, salt-back-titrations are a good method to test the relative binding affinities of UvsX and UvsY, either alone or in combination, for the $12FdT_{24}$ lattice in the presence/absence of various nucleotide ligands of the UvsX protein (ADP, ATPγS, or ATP + regenerating system). The salt-stabilities of the complexes were measured by monitoring the increase in the fluorescence signal of the fluorescein moiety of $12FdT_{24}$ with increasing NaCl concentration. Fluorescence data were converted to fractional saturation of the lattice (θ) values as described in Materials and Methods. Typical salt-back-titration curves are shown in Figure 4. All curves were monophasic in appearance, including those for the UvsX−UvsY−$12FdT_{24}$ complexes, suggesting that UvsX and UvsY dissociate from $12FdT_{24}$ together and not in stages. Therefore, fluorescence data for these tripartite complexes were assigned single θ values representing the global disruption of the complex. The relative stabilities of complexes were determined by comparing the salt concentrations at which $\theta = 0.5$, that is, the amount of salt required to cause 50% dissociation of the complex. These dissociation midpoints were fitted and statistically analyzed as described in Materials and Methods and listed in Table 1.

An inspection of the salt-back-titrations in Figure 4 shows that the UvsY protein causes a large shift in the dissociation of the UvsX−$12FdT_{24}$ complexes to higher NaCl concentrations. These shifts are quantified by the dissociation midpoint values listed in Table 1. The shift was observed under all conditions tested, including the absence of any nucleotide ligand (Figure 4A), the presence of 1 mM ADP (Figure 4B), the presence of 1 mM ATP plus an ATP regenerating system (Figure 4C), and the presence of 1 mM ATPγS (Figure 4D), an ATP analogue that is poorly hydrolyzed by UvsX (Farb, J. and Morrical, S., unpublished experiments). In all cases, the differences between the dissociation midpoints for UvsX versus UvsX + UvsY data sets are statistically significant to a high degree of confidence (Table 2). Likewise, in all cases, the dissociation midpoints for UvsX + UvsY data sets exceed those for UvsY alone, and the differences are statistically significant (Tables 1−2). Therefore, salt-back-titration and ATPase data (Figure 2) both argue that the maximally fluorescence-quenched complex detected in Figure 1 represents a unique UvsX−$12FdT_{24}$ complex that forms in the presence of UvsY, consistent with a tripartite UvsX−UvsY−$12FdT_{24}$ complex. The formation of this complex stabilizes UvsX−ssDNA interactions against the disruption by salt under equilibrium binding conditions as well as steady-state conditions for UvsX-catalyzed, ssDNA-dependent ATP hydrolysis. The effect of UvsY is global and does not depend on UvsX protein binding to a nucleotide ligand.

Salt-back-titration data also reveal a large stabilizing effect of ATPγS on UvsX−$12FdT_{24}$ interactions (Figure 4 and Table 1). In the absence of UvsY, ATPγS increases the dissociation midpoint of UvsX from ~150 to ~470 mM NaCl. Thus, ATPγS induces a strong but reversible binding of UvsX to the short oligonucleotide $12FdT_{24}$, which parallels its effect on UvsX binding to ssDNA−cellulose at low binding density (300-fold increase in observed K_{ss}; reference (*23*)). Other nucleotide ligands have less pronounced effects on UvsX−$12FdT_{24}$ interactions. But surprisingly, ADP appears to moderately stabilize UvsX−$12FdT_{24}$, increasing the dissociation midpoint from ~150 to ~250 mM NaCl in the absence of UvsY, a statistically significant change. ATP (with a regenerating system) has a smaller effect, increasing the midpoint to ~200 mM NaCl in the absence of UvsY.

Salt-back-titration data indicate that UvsY generally forms more stable complexes with $12FdT_{24}$ than does UvsX, except in the presence of ATPγS, wherein UvsX forms the more stable bipartite complex (Table 1). The relative affinities of UvsX and UvsY for $12FdT_{24}$ parallel those observed with other single-stranded lattices (*28*, *32*). UvsY lacks nucleotide binding activity; therefore, as expected, UvsY−$12FdT_{24}$ interactions appear to be independent of nucleotides. UvsY−$12FdT_{24}$ dissociation midpoints range from ~290−380 mM NaCl in our experiments, with a global average of 330 ± 40 mM NaCl.

A key finding of the salt-back-titration experiments is that the stabilizing effects of UvsY and ATPγS on UvsX−$12FdT_{24}$ interactions are synergistic (Figure 4, Table 1). Thus, although ATPγS and UvsY produce qualitatively similar

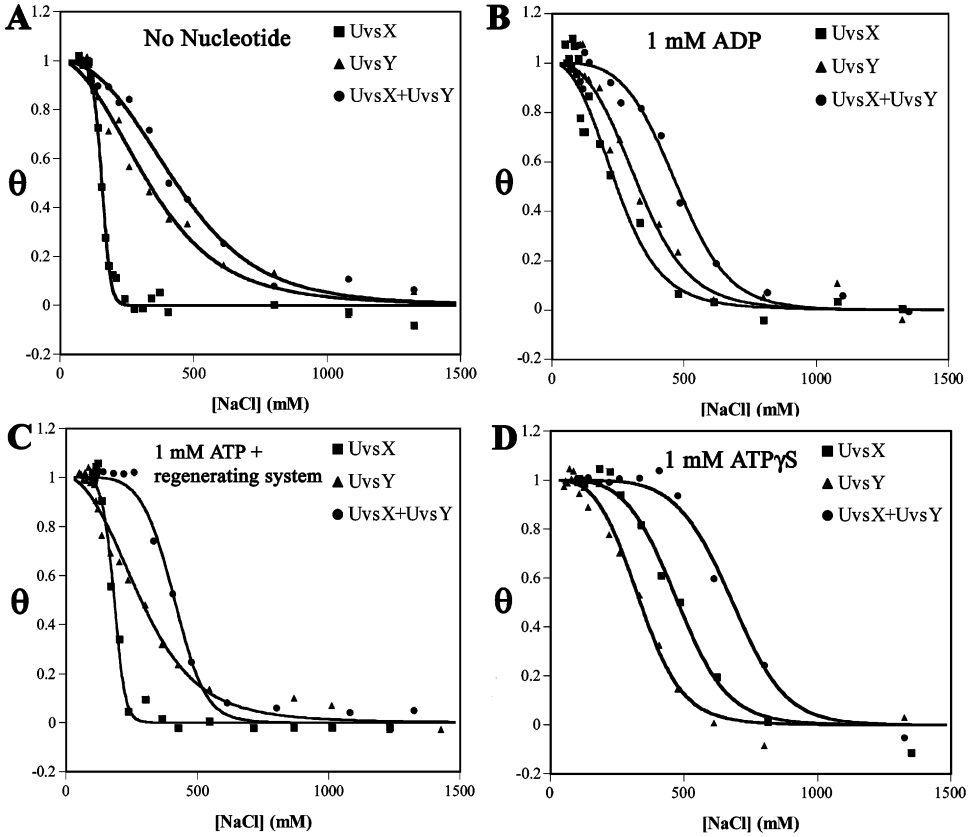

FIGURE 4: Salt-back-titrations of preformed UvsX-, UvsY-, and UvsX−UvsY−12FdT$_{24}$ complexes in the presence/absence of the nucleotide ligands of UvsX protein. Fluorescence measurements and salt-back-titrations were performed as described in Materials and Methods. All reactions contained buffer A and a starting concentration of 100 mM NaCl and (A) no nucleotide, (B) 1 mM ADP, (C) 1 mM ATP + regenerating system, or (D) 1 mM ATPγS. All reactions contained 2 μM 12FdT$_{24}$ and 0.5 μM UvsX (■), 0.5 μM UvsY (▲), or 0.5 μM UvsX + 0.5 μM UvsY (●). Curve fitting and extraction of dissociation midpoints were performed as described in Materials and Methods.

Table 1: Salt-back Titration Dissociation Midpoints for 12FdT$_{24}$ Complexes with UvsX Alone, UvsY Alone, or Both UvsX and UvsY, in the Presence and Absence of Different Nucleotides[a]

	dissociation midpoint (mM NaCl)		
cofactor	UvsX	UvsY	UvsX + UvsY
no cofactor	153 ± 13	377 ± 40	409 ± 66
ADP	248 ± 26	343 ± 24	531 ± 48
ATP + R.S.[b]	200 ± 39	292 ± 10	395 ± 31
ATPγS	467 ± 31	323 ± 40	755 ± 136

[a] All data were derived from computer fits of salt-back-titration curves as shown in Figure 4 and as described in Materials and Methods. Each value represents the average (±standard deviation) from three different experiments. [b] ATP + R.S. denotes data sets for reactions containing ATP and the regenerating system.

Table 2: Wilcoxon Rank Sum Test and Student's t-Test Results Comparing Salt-Back-Titration Dissociation Midpoints from Table 1

	data	test	Wilcoxon[a]	t-test
A[d]	UvsX	+ATPγS vs −ATPγS	6.993×10^{-3}	3.872×10^{-7}
B	UvsX+UvsY	+ATPγS vs −ATPγS	1.998×10^{-3}	2.229×10^{-3}
C	+ATPγS[b]	UvsX vs UvsX + UvsY	5.714×10^{-2}	7.200×10^{-3}
D	−ATPγS[c]	UvsX vs UvsX + UvsY	1.083×10^{-5}	8.483×10^{-8}
E	UvsY	+UvsX vs −UvsX	2.713×10^{-4}	1.138×10^{-3}

[a] Wilcoxon and t-test values represent probabilities that the compared data are statistically the same. [b] +ATPγS denotes data sets for reactions containing ATPγS. [c] −ATPγS denotes all other ligand conditions (ADP, ATP + regenerating system, and no nucleotide). [d] A. A comparison between the dissociation midpoints of the UvsX−12FdT$_{24}$ complex in the presence of ATPγS (+ATPγS) vs all other conditions (−ATPγS). B. A comparison between the dissociation midpoints of the UvsX−UvsY−12FdT$_{24}$ complex in the presence of ATPγS (+ATPγS) vs all other conditions (−ATPγS). C. A comparison between the dissociation midpoints of the UvsX−12FdT$_{24}$ vs the UvsX−UvsY−12FdT$_{24}$ complexes in the presence of ATPγS. D. A comparison between the dissociation midpoints of the UvsX−12FdT$_{24}$ vs the UvsX−UvsY−12FdT$_{24}$ complexes under all other ligand conditions (ADP, ATP + regenerating system, and no nucleotide). E. A comparison between the dissociation midpoints of the UvsY−12FdT$_{24}$ vs the UvsX−UvsY−12FdT$_{24}$ complexes under all ligand conditions (ATPγS, ADP, ATP + regenerating system, and no nucleotide).

increases in the salt stability of UvsX−12FdT$_{24}$ interactions (θ = 0.5 at 153, 409, or 467 mM NaCl for UvsX alone, UvsX + UvsY, or UvsX + ATPγS, respectively), their effects are nonredundant because both are required to produce a maximally stabilized presynaptic filament complex (θ = 0.5 at 755 mM NaCl for UvsX + UvsY + ATPγS).

Effects of UvsY Missense Mutants on UvsX−12FdT$_{24}$ Interactions. Two previously characterized UvsY missense mutants, UvsY$_{K58A}$ and UvsY$_{K58A,R60A}$, poorly bind to ssDNA but retain strong interactions with UvsX at moderate NaCl concentrations (*30*). We therefore used these mutants to explore the effects of UvsX−UvsY protein−protein interactions on the stabilization of UvsX−12FdT$_{24}$ complexes. Figure 5A shows the fluorescence spectra of 12FdT$_{24}$ in the presence/absence of UvsY$_{K58A}$ or UvsY$_{K58A,R60A}$, obtained under solution conditions identical to those used for the wild-type UvsY in Figure 1 (100 mM NaCl). Both mutants exhibit reduced quenching of 12FdT$_{24}$ compared to that of the wild-type, suggesting the failure to form stable complexes with the oligo under these conditions. This is confirmed by the observation that in salt-back-titrations of UvsY mutant +

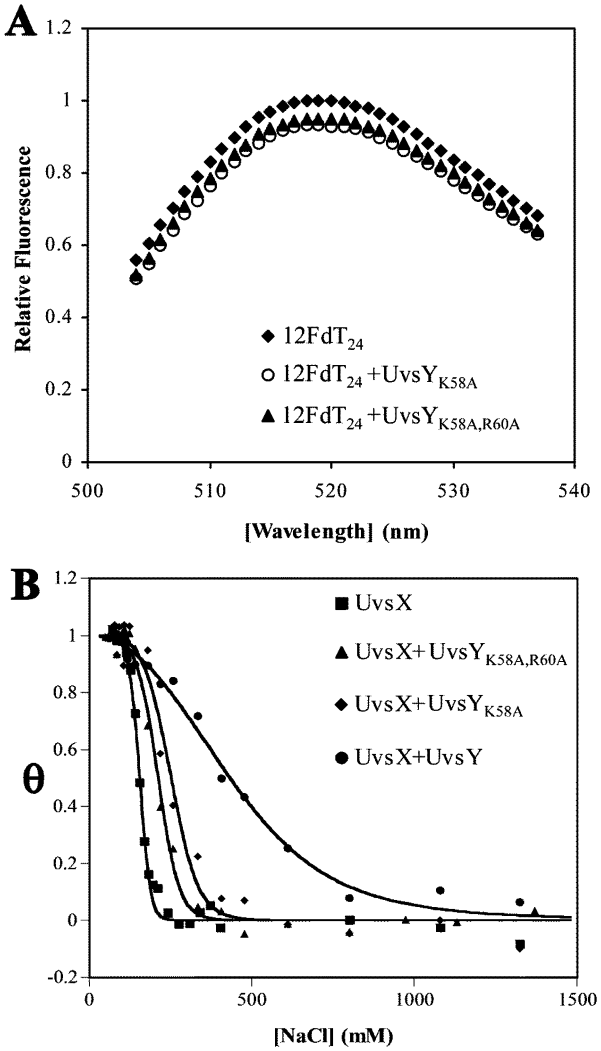

FIGURE 5: (A) Fluorescence spectra of 2 μM 12FdT$_{24}$ alone (♦), with 0.5 μM UvsY$_{K58A}$ (○), and with 0.5 μM UvsY$_{K58A,R60A}$ (▲), all in buffer A + 100 mM NaCl. The fluorescence measurements were performed as described in Materials and Methods. (B) Salt-back-titrations of mixtures containing 2 μM 12FdT$_{24}$, 0.5 μM UvsX (■) and 0.5 μM UvsY$_{K58A}$ (♦), 0.5 μM UvsY$_{K58A,R60A}$ (▲), or 0.5 μM wild-type UvsY (●). All reactions contained buffer A plus a starting concentration of 100 mM NaCl. Curve fitting and extraction of dissociation midpoints were performed as described in Materials and Methods.

12FdT$_{24}$ mixtures, fluorescence quenching is completely abolished above 150 mM NaCl (data not shown). Figure 5B shows salt-back-titrations of UvsX−12FdT$_{24}$ complexes in the presence/absence of UvsY$_{K58A}$, UvsY$_{K58A,R60A}$, or wild-type UvsY. The dissociation midpoints of these titrations are listed in Table 3 and statistically analyzed in Table 4. It is clear that the UvsY mutants have greatly reduced abilities to stabilize UvsX−12FdT$_{24}$ complexes against increasing salt concentrations, with the greater defect occurring in the double missense mutant UvsY$_{K58A,R60A}$ (Figure 5B, Table 3). The K58A and K58A,R60A mutations do not completely abolish the stabilizing effect of UvsY on UvsX−12FdT$_{24}$ interactions, however, because both mutants afford a statistically significant increase in the dissociation midpoint compared to that with UvsX alone (Tables 3 and 4). Midpoint statistics also confirm that the stabilization effects of UvsY$_{K58A}$, UvsY$_{K58A,R60A}$, and wild-type UvsY are different from each other to a high degree of confidence (Table 4). Because

Table 3: Salt-Back-Titration Dissociation Midpoints for 12F-dT$_{24}$ Complexes with UvsX ± UvsY$_{K58A}$, UvsY$_{K58A,\ R60A}$, or UvsY Wild Type in the Absence of Nucleotide Ligands[a]

	dissociation midpoint (mM NaCl)			
	UvsX	UvsX + UvsY$_{K58A}$	UvsX + UvsY$_{K58A,R60A}$	UvsX + UvsY
no cofactor	153 ± 13	242 ± 16	216 ± 4	409 ± 66

[a] All data were derived from computer fits of salt-back-titration curves as shown in Figure 5 and as described in Materials and Methods. Each value represents the average (± standard deviation) from three different experiments.

Table 4: Wilcoxon Rank Sum Test and Student's t-Test Results Comparing Salt-Back-Titration Dissociation Midpoints from Table 3

data test	Wilcoxon[a]	t-test[a]
UvsX + UvsY vs UvsX + UvsY$_{K58A}$	9.524×10^{-3}	4.300×10^{-3}
UvsX + UvsY vs UvsX + UvsY$_{K58A,R60A}$	9.524×10^{-3}	4.013×10^{-3}
UvsX vs UvsX + UvsY$_{K58A}$	2.381×10^{-2}	3.973×10^{-3}
UvsX vs UvsX + UvsY$_{K58A,R60A}$	2.381×10^{-2}	1.622×10^{-2}
UvsX + UvsY$_{K58A}$ vs UvsX + UvsY$_{K58A,R60A}$	1.515×10^{-2}	1.773×10^{-2}

[a] Wilcoxon and t-test values represent probabilities that the compared data are statistically the same.

dissociation midpoints obtained with both mutants exceed 200 mM NaCl (Table 3), a salt concentration at which ssDNA-binding activity for both should be minimal to nonexistent (*23*, *30*), we conclude that protein−protein interactions between UvsY mutants and UvsX account for the residual stabilization effects.

DISCUSSION

The fluorescent oligonucleotide 12FdT$_{24}$ is a useful probe for studying protein−ssDNA interactions that are important for bacteriophage T4 presynaptic filament assembly and function. UvsX recombinase and its RMP partner, UvsY, both bind to 12FdT$_{24}$ and differentially quench the fluorescence of its fluorescein moiety. 12FdT$_{24}$ is a sufficient lattice to activate the ssDNA-dependent ATPase activity of UvsX, and the well-documented stimulation of this activity by UvsY (*16*, *17*) is recapitulated. Most importantly, for this study, the changes in 12FdT$_{24}$ fluorescence allow the measurements of the effects of UvsY on UvsX−ssDNA interactions. The addition of UvsX to preformed UvsY−12FdT$_{24}$ results in a maximally fluorescence-quenched complex that contains both UvsX and UvsY bound to oligo as evidenced by: (1) the activation of UvsX ATPase activity; (2) a UvsY-signature red shift in the λ_{max} of 12FdT$_{24}$ fluorescence; and (3) a UvsY-dependent enhancement of both the ATPase activity and salt-stability of the complex. The properties of the tripartite UvsX−UvsY−12FdT$_{24}$ complex detected by our fluorescence assay system are consistent with properties of UvsX−UvsY−ssDNA recombination intermediates inferred by previous studies (*25*, *27*, *39*) so that quantitative information revealed herein is highly relevant to the mechanisms of presynaptic filament assembly and DNA strand exchange in the T4 system. Previous EM studies revealed that UvsX forms extended helical filaments nearly identical to those formed by *E. coli* RecA protein (*40*, *41*). The extended nucleofilaments of UvsX on both ss- and ds-DNA have mean

pitches of 90−95 Å and ~19 bases or base-pairs per helical turn, representing a 5 Å axial rise per base or bp (*40*). In addition, EM and crystallographic reconstructions of T4, *E. coli*, and yeast presynaptic filaments indicate an ~6-fold pseudorotational symmetry of subunits around the filament screw axis (*42*−*44*). Therefore, the oligo $12FdT_{24}$ used in our studies, containing six binding sites for UvsX and/or UvsY protomers, supports at least one helical turn of the filament at saturation. The 24-mer binds to one UvsY hexamer (*31*), allowing the study of UvsX interactions with the minimal UvsY−ssDNA complex.

Previous studies showed that UvsY allows UvsX to catalyze reactions such as ssDNA-dependent ATP hydrolysis and DNA strand exchange at higher salt and/or at lower UvsX concentrations, suggesting that UvsY stabilizes UvsX−ssDNA presynaptic filaments (*16*, *25*, *45*). Our results confirm that UvsY stabilizes UvsX−ssDNA interactions against disruption by salt and demonstrate that this effect reflects a global increase in the apparent equilibrium binding affinity, represented by $K_{ss}\omega$, of UvsX for ssDNA. Other results suggest that UvsY does not affect the cooperativity parameter, ω, of UvsX (Liu, J. and Morrical, S., unpublished experiments). Therefore, UvsY appears to act by specifically increasing the intrinsic affinity parameter, K_{ss}, of UvsX for ssDNA. The increase in K_{ss} does not require a specific nucleotide-liganded form of the UvsX protein because UvsY stabilizes complexes in the presence/absence of ADP or ATPγS under equilibrium conditions and also stabilizes complexes under steady-state conditions for ATP hydrolysis.

Missense mutants $UvsY_{K58A}$ and $UvsY_{K58A,R60A}$ have dramatically reduced affinities for ssDNA compared to that of wild-type UvsY but retain self and heteroassociation properties similar to those of the wild-type (*30*). Both mutants show a greatly reduced ability to stabilize UvsX−$12FdT_{24}$ interactions in salt-back-titrations. This finding indicates that UvsY−ssDNA interactions play a major role in stabilizing UvsX−ssDNA interactions. Because the evidence suggests that the high-affinity binding of UvsY to ssDNA is mediated by the wrapping of the polynucleotide around the UvsY hexamers (*27*, *31*, *46*), it is probable that the wrapping or a related ssDNA structural change brought about by UvsY creates an optimal lattice for high-affinity UvsX−ssDNA interactions. A model for this process is schematically shown in Figure 6. It is also possible that the UvsX−UvsY protein−protein interactions are synergistically enhanced within the wild-type complex and that this enhancement contributes to the increased salt-stability of the complex. The residual stabilization effects seen with $UvsY_{K58A}$ and $UvsY_{K58A,R60A}$ (Figure 5, Table 3) are likely the result of the UvsY−UvsX protein−protein interactions because the experiments were carried out at salt and protein concentrations that abrogate ssDNA binding by the mutants (*30*). A relatively weak stabilization effect caused by the protein−protein interactions between UvsY mutants and UvsX may explain why these mutants are only partially defective in stimulating UvsX's ssDNA-dependent ATPase and DNA strand exchange activities (*30*).

ATPγS strongly stabilizes UvsX−$12FdT_{24}$ interactions, but complex formation is reversible at moderate NaCl concentrations (Figure 4, Table 1). This observation contrasts with the effect of ATPγS on long UvsX−ϵDNA filaments, which are stable at salt concentrations exceeding 1 M NaCl or 1.3 M NaOAc (*32*). The amplified effect of ATPγS on long filaments suggests that in addition to increasing the intrinsic binding affinity (K_{ss}) of UvsX for ssDNA ATPγS may also stabilize cooperative interactions between neighboring UvsX monomers. UvsX−$12FdT_{24}$ complexes are also moderately stabilized by ADP, whereas the long UvsX−ϵDNA filaments were not affected by ADP (*32*). The difference may be due to the different lattices used, or it may reflect the differences between short, nucleation-like complexes versus long mature filaments. Further experiments will be needed to resolve this issue.

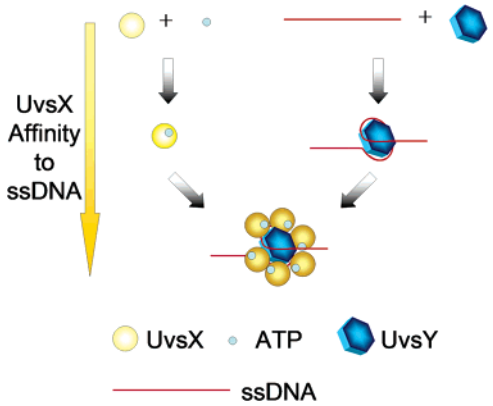

FIGURE 6: Model for the roles of UvsY and ATP in the nucleation of UvsX−ssDNA presynaptic filaments. UvsY binding induces a structural change in ssDNA that may involve the wrapping of the polynucleotide around a UvsY hexamer (*12*, *27*, *31*). UvsX binds with high affinity to the UvsY−ssDNA complex. ATP binding independently enhances the affinity of UvsX for ssDNA, and the effect is synergistic with the UvsY-mediated stabilization of UvsX−ssDNA interactions so that the combination of ATP and UvsY effects results in a maximally stabilized complex. ssDNA-stimulated ATP hydrolysis by UvsX causes the nucleotide-mediated stabilization to be transient, but UvsY-mediated stabilization is independent of the nucleotide, allowing a stabilized nucleation complex to persist through the catalytic cycle. The cartoon represents a minimal UvsX−UvsY−ssDNA complex involving a single UvsY hexamer, such as may occur during filament nucleation. Similar interactions may occur at many sites throughout the longer presynaptic filament.

A key finding of this study is that the stabilizing effects of UvsY and ATPγS on UvsX−ssDNA interactions are synergistic. Individually, both factors are capable of inducing a high-affinity ssDNA binding form of UvsX but by nonredundant mechanisms (Figure 6). The synergistic effects of ATPγS binding and UvsY apply not only to the short UvsX−$12FdT_{24}$ complex but also to the UvsX−ssDNA complexes formed on natural M13mp18 ssDNA (Liu, J. and Morrical, S., unpublished experiments), which argues that results obtained with short oligo lattices are biologically relevant. ATPγS and UvsY may affect different components of the UvsX−ssDNA interactions, that is, affinity versus cooperativity parameters and electrostatic versus nonelectrostatic elements of binding. The synergistic effects of UvsY and ATPγS have important implications for targeting UvsX recombinase assembly onto ssDNA under physiological conditions in which dsDNA is present in large excess (*23*).

Wrapping or related ssDNA structural changes brought about by UvsY are also implicated in the destabilization of Gp32−ssDNA interactions observed in tripartite UvsY−Gp32−ssDNA complexes that are intermediates in DNA strand exchange (*25*, *27*, *39*). Thus, there is linkage between the UvsY-mediated destabilization of Gp32−ssDNA and the

stabilization of UvsX−ssDNA interactions. This suggests a seamless progression from a preexisting Gp32−ssDNA complex to a UvsY−Gp32−ssDNA intermediate to a UvsY- and nucleoside triphosphate-stabilized nucleation complex with ssDNA structural change as the common denominator. The ejection of Gp32 from the nascent filament may be an active process that is coupled to the recruitment of UvsX and/or ATP binding and hydrolysis by the recombinase. Alternatively, a passive mechanism may apply wherein UvsX (with $K_{ss}\omega$ increased by UvsY and nucleoside triphosphate) simply out-competes Gp32 (with $K_{ss}\omega$ decreased by UvsY) for binding sites on ssDNA. Further experimentation is required to resolve between these models.

It is evident from these and related studies that presynaptic filament assembly involves a delicate interplay between the DNA binding properties and protein−protein interactions of recombinase, ssDNA-binding protein, and recombination mediator protein components. The inhibition of presynaptic filament assembly by dsDNA and SSBs is a problem encountered by most recombination systems; therefore, it is possible that many RMP factors function at least in part by stabilizing recombinase−ssDNA interactions. Further mechanistic studies of presynaptic filament stabilization in T4 and other recombination systems will be critical for understanding the dynamics of these structures in homologous recombination transactions.

ACKNOWLEDGMENT

We thank Dr. Jill S. Bleuit for providing two UvsY mutant proteins and Dr. Christopher Berger for the use of his fluorometer.

REFERENCES

1. Formosa, T., and Alberts, B. M. (1986) DNA synthesis dependent on genetic recombination: characterization of a reaction catalyzed by purified bacteriophage T4 proteins, *Cell 47*, 793−806.
2. Kreuzer, K. N. (2000) Recombination-dependent DNA replication in phage T4, *Trends Biochem. Sci. 25*, 165−173.
3. Bleuit, J. S., Xu, H., Ma, Y., Wang, T., Liu, J., and Morrical, S. W. (2001) Mediator proteins orchestrate enzyme-ssDNA assembly during T4 recombination-dependent DNA replication and repair, *Proc. Natl. Acad. Sci. U.S.A. 98*, 8298−8305.
4. Bianco, P. R., Tracy, R. B., and Kowalczykowski, S. C. (1998) DNA strand exchange proteins: a biochemical and physical comparison, *Front. Biosci. 3*, D570−603.
5. Kowalczykowski, S. C., Dixon, D. A., Eggleston, A. K., Lauder, S. D., and Rehrauer, W. M. (1994) Biochemistry of homologous recombination in *Escherichia coli*, *Microbiol. Rev. 58*, 401−465.
6. Symington, L. S. (2002) Role of RAD52 epistasis group genes in homologous recombination and double-strand break repair, *Microbiol. Mol. Biol. Rev. 66*, 630−670.
7. Moynahan, M. E., Cui, T. Y., and Jasin, M. (2001) Homology-directed DNA repair, mitomycin-c resistance, and chromosome stability is restored with correction of a Brca1 mutation, *Cancer Res. 61*, 4842−4850.
8. Yu, V. P., Koehler, M., Steinlein, C., Schmid, M., Hanakahi, L. A., van Gool, A. J., West, S. C., and Venkitaraman, A. R. (2000) Gross chromosomal rearrangements and genetic exchange between nonhomologous chromosomes following BRCA2 inactivation, *Genes Dev. 14*, 1400−1406.
9. Scully, R. (2000) Role of BRCA gene dysfunction in breast and ovarian cancer predisposition, *Breast Cancer Res. 2*, 324−330.
10. Jasin, M. (2002) Homologous repair of DNA damage and tumorigenesis: the BRCA connection, *Oncogene 21*, 8981−8993.
11. Pierce, A. J., Stark, J. M., Araujo, F. D., Moynahan, M. E., Berwick, M., and Jasin, M. (2001) Double-strand breaks and tumorigenesis, *Trends Cell Biol. 11*, S52−59.
12. Beernink, H. T., and Morrical, S. W. (1999) RMPs: recombination/replication mediator proteins, *Trends Biochem. Sci. 24*, 385−389.
13. New, J. H., Sugiyama, T., Zaitseva, E., and Kowalczykowski, S. C. (1998) Rad52 protein stimulates DNA strand exchange by Rad51 and replication protein A, *Nature 391*, 407−410.
14. Shinohara, A., and Ogawa, T. (1998) Stimulation by Rad52 of yeast Rad51-mediated recombination, *Nature 391*, 404−407.
15. Sung, P. (1997) Yeast Rad55 and Rad57 proteins form a heterodimer that functions with replication protein A to promote DNA strand exchange by Rad51 recombinase, *Genes Dev. 11*, 1111−1121.
16. Harris, L. D., and Griffith, J. D. (1989) UvsY protein of bacteriophage T4 is an accessory protein for in vitro catalysis of strand exchange, *J. Mol. Biol. 206*, 19−27.
17. Yonesaki, T., and Minagawa, T. (1989) Synergistic action of three recombination gene products of bacteriophage T4, uvsX, uvsY, and gene 32 proteins, *J. Biol. Chem. 264*, 7814−7820.
18. Umezu, K., Chi, N. W., and Kolodner, R. D. (1993) Biochemical interaction of the *Escherichia coli* RecF, RecO, and RecR proteins with RecA protein and single-stranded DNA binding protein, *Proc. Natl. Acad. Sci. U.S.A. 90*, 3875−3879.
19. Umezu, K., and Kolodner, R. D. (1994) Protein interactions in genetic recombination in *Escherichia coli*. Interactions involving RecO and RecR overcome the inhibition of RecA by single-stranded DNA-binding protein, *J. Biol. Chem. 269*, 30005−30013.
20. Baumann, P., and West, S. C. (1997) The human Rad51 protein: polarity of strand transfer and stimulation by hRP-A, *EMBO J. 16*, 5198−5206.
21. Namsaraev, E. A., and Berg, P. (1998) Binding of Rad51p to DNA. Interaction of Rad51p with single- and double-stranded DNA, *J. Biol. Chem. 273*, 6177−6182.
22. Sung, P., and Robberson, D. L. (1995) DNA strand exchange mediated by a RAD51-ssDNA nucleoprotein filament with polarity opposite to that of RecA, *Cell 82*, 453−461.
23. Xu, H. (2005) Biochemical and structural characterization of bacteriophage T4 recombination/replication mediator proteins, pp 260, University of Vermont, Burlington, VT.
24. Formosa, T., and Alberts, B. M. (1986) Purification and characterization of the T4 bacteriophage uvsX protein, *J. Biol. Chem. 261*, 6107−6118.
25. Kodadek, T., Gan, D. C., and Stemke-Hale, K. (1989) The phage T4 uvsY recombination protein stabilizes presynaptic filaments, *J. Biol. Chem. 264*, 16451−16457.
26. Griffith, J., and Formosa, T. (1985) The UvsX protein of bacteriophage T4 arranges single-stranded and double-stranded DNA into similar helical nucleoprotein filaments, *J. Biol. Chem. 260*, 4484−4491.
27. Sweezy, M. A., and Morrical, S. W. (1999) Biochemical interactions within a ternary complex of the bacteriophage T4 recombination proteins uvsY and gp32 bound to single-stranded DNA, *Biochemistry 38*, 936−944.
28. Sweezy, M. A., and Morrical, S. W. (1997) Single-stranded DNA binding properties of the UvsY recombination protein of bacteriophage T4, *J. Mol. Biol. 266*, 927−938.
29. Yassa, D. S., Chou, K. M., and Morrical, S. W. (1997) Characterization of an amino-terminal fragment of the bacteriophage T4 uvsY recombination protein, *Biochimie 79*, 275−285.
30. Bleuit, J. S., Ma, Y., Munro, J., and Morrical, S. W. (2004) Mutations in a conserved motif inhibit single-stranded DNA binding and recombination mediator activities of bacteriophage T4 UvsY protein, *J. Biol. Chem. 279*, 6077−6086.
31. Beernink, H. T., and Morrical, S. W. (1998) The uvsY recombination protein of bacteriophage T4 forms hexamers in the presence and absence of single-stranded DNA, *Biochemistry 37*, 5673−5681.
32. Ando, R. A., and Morrical, S. W. (1998) Single-stranded DNA binding properties of the UvsX recombinase of bacteriophage T4: binding parameters and effects of nucleotides, *J. Mol. Biol. 283*, 785−796.
33. Yonesaki, T., and Minagawa, T. (1985) T4 phage gene uvsX product catalyzes homologous DNA pairing, *EMBO J. 4*, 3321−3327.
34. Morrical, S. W., Hempstead, K., and Morrical, M. D. (1994) The gene 59 protein of bacteriophage T4 modulates the intrinsic and single-stranded DNA-stimulated ATPase activities of gene 41 protein, the T4 replicative DNA helicase, *J. Biol. Chem. 269*, 33069−33081.
35. Birdsall, B., King, R. W., Wheeler, M. R., Lewis, C. A., Jr., Goode, S. R., Dunlap, R. B., and Roberts, G. C. (1983) Correction for light absorption in fluorescence studies of protein−ligand interactions, *Anal. Biochem. 132*, 353−361.

36. Lefebvre, S. D., and Morrical, S. W. (1997) Interactions of the bacteriophage T4 gene 59 protein with single-stranded polynucleotides: binding parameters and ion effects, *J. Mol. Biol. 272*, 312−326.
37. Team, R. D. C. (2004) *R: A language and environment for statistical computing*. R foundation for statistical computing, Vienna, Austria.
38. Hashimoto, K., and Yonesaki, T. (1991) The characterization of a complex of three bacteriophage T4 recombination proteins, uvsX protein, uvsY protein, and gene 32 protein, on single-stranded DNA, *J. Biol. Chem. 266*, 4883−4888.
39. Jiang, H., Giedroc, D., and Kodadek, T. (1993) The role of protein−protein interactions in the assembly of the presynaptic filament for T4 homologous recombination, *J. Biol. Chem. 268*, 7904−7911.
40. Yu, X., and Egelman, E. H. (1993) DNA conformation induced by the bacteriophage T4 UvsX protein appears identical to the conformation induced by the *Escherichia coli* RecA protein, *J. Mol. Biol. 232*, 1−4.
41. Yu, X., Jacobs, S. A., West, S. C., Ogawa, T., and Egelman, E. H. (2001) Domain structure and dynamics in the helical filaments formed by RecA and Rad51 on DNA, *Proc. Natl. Acad. Sci. U.S.A. 98*, 8419−8424.
42. Conway, A. B., Lynch, T. W., Zhang, Y., Fortin, G. S., Fung, C. W., Symington, L. S., and Rice, P. A. (2004) Crystal structure of a Rad51 filament, *Nat. Struct. Mol. Biol. 11*, 791−796.
43. Story, R. M., and Steitz, T. A. (1992) Structure of the recA protein-ADP complex, *Nature 355*, 374−376.
44. Story, R. M., Weber, I. T., and Steitz, T. A. (1992) The structure of the *E. coli* recA protein monomer and polymer, *Nature 355*, 318−325.
45. Morrical, S. W., and Alberts, B. M. (1990) The UvsY protein of bacteriophage T4 modulates recombination-dependent DNA synthesis in vitro, *J. Biol. Chem. 265*, 15096−15103.
46. Ando, R. A., and Morrical, S. W. (1999) Relationship between hexamerization and ssDNA binding affinity in the uvsY recombination protein of bacteriophage T4, *Biochemistry 38*, 16589−16598.

BI0525167